OPEN ACCESS
JOURNAL OF ADVANCED DIELECTRICS
Vol. 11, No. 6 (2021) 2150025 (6 pages)

DOI: 10.1142/S2010135X21500259

Electrical transport properties of V_2O_5-added Ni–Co–Zn ferrites

M. Firoz Uddin[*], M. Samir Ullah[*,¶], S. Manjura Hoque[‡], F. A. Khan[*], A. A. Momin[§], Sm. Rubayatul Islam[*], Faizus Salehin[*] and M. A. Hakim[†]

[*]*Department of Physics, Bangladesh University of Engineering and Technology Dhaka 1000, Bangladesh*

[†]*Department of Glass and Ceramic Engineering Bangladesh University of Engineering and Technology, Dhaka 1000, Bangladesh*

[‡]*Materials Science Division, Atomic Energy Center, Dhaka 1000, Bangladesh*

[§]*Department of Physics, Jagannath University, Dhaka 1100, Bangladesh*

[¶]samirullah@phy.buet.ac.bd

Received 28 June 2021; Revised 23 August 2021; Accepted 17 September 2021; Published 18 November 2021

Frequency-dependent dielectric constant, dielectric loss, AC conductivity values and complex impedance spectra of V_2O_5-added Ni–Co–Zn ferrites ($Ni_{0.62}Co_{0.03}Zn_{0.35}Fe_2O_4 + xV_2O_5$, where x = 0, 0.5, 1 and 1.5 wt.%) have been investigated at room temperature. The dielectric properties of the samples follow the Maxwell–Wagner polarization model. An inverse relationship was found between dielectric constant and AC electrical resistivity for all the samples. The dielectric constants decreased with the addition of V_2O_5, while the electrical resistivities of V_2O_5-added Ni–Co–Zn ferrites are found to be larger than that of pure Ni–Co–Zn ferrite. The AC conductivity was reduced with the addition of V_2O_5 to Ni–Co–Zn ferrite at lower-frequency region. However, AC conductivity shows a sharp increase at higher-frequency region, which could be attributed to the enhancement of electron hopping between the Fe^{2+} and Fe^{3+} ions in the ferrite matrix due to the activity of the grains. The complex impedance spectroscopy results through Cole–Cole/Nyquist plot have demonstrated a single semicircular arc. It indicates that conduction mechanism takes place predominantly through the grain/bulk property, which could be ascribed to the larger grain size of V_2O_5-added Ni–Co–Zn ferrites.

Keywords: Dielectric constant; electrical resistivity; AC conductivity; complex impedance; Cole–Cole plot.

1. Introduction

Soft spinel ferrites are ferrimagnetic materials which have significant role in different types of electromagnetic devices.[1–6] Ni–Zn mixed ferrite is one of the important magnetic materials which have been used in electronic industries as well as communications technology.[7–9] On the other hand, Ni–Co–Zn mixed ferrites are used in electromagnetic devices for their significant magnetic anisotropy and chemical stability.[10,11] The dielectric properties of the spinel ferrites are strongly dependent on the crystal structure, cation distribution, chemical compositions, grain structure, preparation method, sintering temperature and types of substitution or additives.[12,13] There are different types of additives such as V_2O_5, MoO_3, Bi_2O_3 and WO_3 which can play significant roles as sintering aids, in microstructure modification, in controlled grain growth and in the densification of the samples.[14–16] It is observed that V_2O_5 has been used as an excellent sintering aid in order to promote grain growth of the ferrite materials.[17] Previously, Lebourgeois *et al*. studied the effects of V_2O_5 additive on the magnetic properties of Ni–Cu–Zn ferrites.[18] They found that V_2O_5 additive can play an important role in the improvement of microstructure of Ni–Cu–Zn ferrites, which influenced the magnetic properties. On the other hand, Kaiser[19] observed the influence of V_2O_5 addition on the conductivity and grain growth of Ni–Zn–Cu ferrites. They studied the AC conductivity and complex impedance spectra in order to understand the conduction mechanism through grain effect. Rao *et al*. observed the influence of V_2O_5 addition on the resistivity and dielectric properties of Ni–Zn ferrites.[20] Jain *et al*. also studied the influence of V_2O_5 addition on the electrical conductivity and magnetic properties of Ni–Zn ferrites.[21] However, they did not study the complex impedance spectroscopy results through Cole–Cole/Nyquist plot in order to know the information about the electrical conduction mechanism of the materials. In addition, a ternary compound with Ni–Co–Zn ferrites having the chemical formula of $Ni_{0.62}Co_{0.03}Zn_{0.35}Fe_2O_4$ has not been studied with V_2O_5 addition. Moreover, this composition has been chosen based on the opposite nature of magnetic anisotropy energies of $CoFe_2O_4$ and $NiFe_2O_4$ that might have a compensating effect on the anisotropy constant of mixed ferrites. There is a lack of data on the effects of V_2O_5 addition on the dielectric constant, AC conductivity and complex impedance spectra of Ni–Co–Zn ferrites. In this work, an attempt has been made to study

[¶]Corresponding author.

in detail the frequency-dependent dielectric constant, dielectric loss, AC conductivity and complex impedance spectra of V_2O_5-added Ni–Co–Zn ferrites.

2. Materials and Method

In order to synthesize the Ni–Co–Zn ferrites, the chemical reagents namely NiO, CoO, ZnO and Fe_2O_3 powders in appropriate amounts were weighed and mixed properly in a ceramic mortar with pestle for 5 h. The grinded powders were pre-sintered at 850 °C for 3 h to form Ni–Co–Zn ferrites through the solid-state reaction technique. Different proportions of V_2O_5 (0.5, 1 and 1.5 wt.%) were added to the calcined powders of Ni–Co–Zn ferrites. Then the V_2O_5-added Ni–Co–Zn ferrite samples were pressed in hydraulic press to form disk-shaped samples. The samples were sintered at 1200 °C temperature in air for 3 h. The dielectric constant and complex impedance spectra for all the synthesized samples were measured using an impedance analyzer (WAYNE KERR 6500B) in the frequency range from 100 Hz to 10 MHz at room temperature. The dielectric constant was calculated from the relation: $\varepsilon' = \frac{C_m d}{\varepsilon_o A}$, where C_m is the capacitance, A is the area of the surface, d is the thickness of the specimen and ε_0 is the permittivity of free space. The complex impedance Z^* is given by: $Z^* = Z' + Z''$, where Z' and Z'' are the real (resistive) and imaginary (reactive) components, respectively. The Cole–Cole/Nyquist plot is a plot between Z' and Z'', expressed by the equation: $(Z' - \frac{R}{2})^2 + (Z'')^2 = (\frac{R}{2})^2$, where $(\frac{R}{2})$ generally represents the radius of semicircle.

3. Results and Discussion

X-ray diffraction (XRD) was used to study the crystal structure. It was confirmed from Fig. 1 that all the samples have cubic spinel crystalline structure with the manifestation of (111), (220), (311), (222), (400), (422), (511) and (440) planes.[22] A detailed microstructural study has been performed using field-emission scanning electron microscopy (FESEM) that demonstrated the nature of grain growth of Ni–Co–Zn ferrites. The grain size of the sintered samples (at the temperature of T_S = 1200 °C) was found to be strongly dependent on V_2O_5 contents and had been reported in our earlier work.[37] The porosity of the samples decreased with the addition of V_2O_5 content, which can be attributed to the role of V_2O_5 as a sintering aid to enhance the densification of the ferrite samples from 4.13 g/cm^3 (for x = 0 wt.% of V_2O_5) to 5 g/cm^3 (for x = 1.5 wt.% of V_2O_5). It clearly demonstrates that V_2O_5 addition can promote grain growth as a sintering aid during the sintering process. The effect of V_2O_5 addition as a sintering aid has been clearly reflected with the concomitant achievement of high density of ferrite materials.

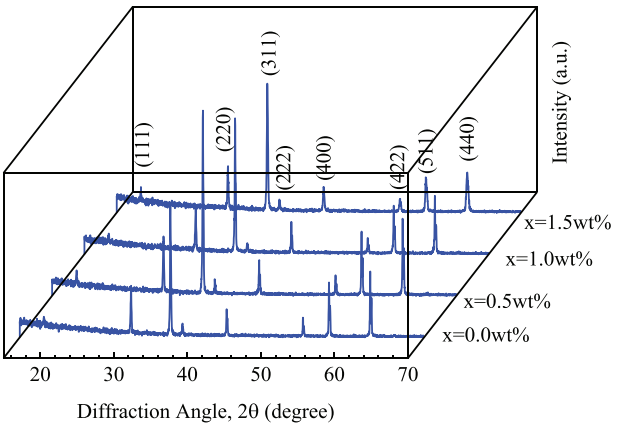

Fig. 1. XRD patterns in three dimensions.

3.1. *Dielectric constant*

Figure 2 shows the variations of the dielectric constant (ε') with applied frequency for different concentrations of V_2O_5-added Ni–Co–Zn ferrites at room temperature. It is observed that ε' decreases with the increase of frequency and attains a constant value at high-frequency region. According to the Maxwell–Wagner type of polarization, ferrites contain good conducting grains separated by poorly conducting grain boundaries.[23] The dielectric constant (ε') of ferrite possessed different types of polarizations such as interfacial, atomic, dipolar and electronic polarizations. All types of polarizations (electronic, ionic and space charge) contribute to ε' at the lower-frequency region, while the effective polarization is only electronic that takes place in the higher-frequency region. The dielectric constants of all the studied samples decrease monotonically as the frequency increases, which is a normal behavior of frequency-dependent dielectrics. It is observed from Fig. 2 that the rate of change of dielectric constant with frequency of V_2O_5-added samples clearly demonstrates a slow decreasing trend compared with pure

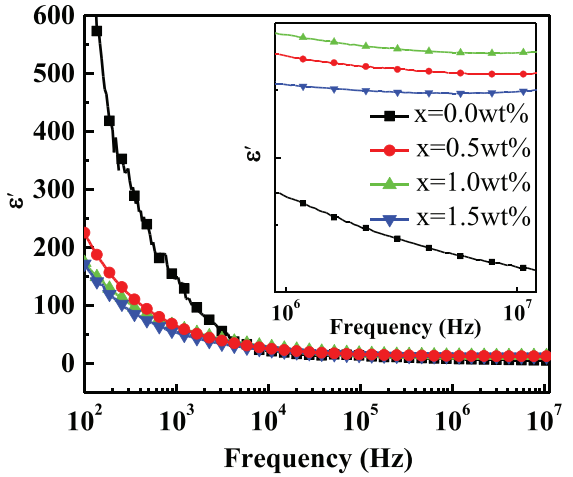

Fig. 2. Variations of the dielectric constant (ε') with applied frequency.

Ni–Co–Zn ferrites. Even at higher frequency, V_2O_5-added Ni–Co–Zn ferrite samples have shown an almost frequency-independent nature, while the pure Ni–Co–Zn ferrites displayed a frequency-dependent behavior as depicted in Fig. 2 (inset). Therefore, it is assumed that V_2O_5-added samples display higher frequency stability than that of pure system. From the FESEM (microstructure) study,[37] the grain growth of Ni–Co–Zn ferrites is dependent on the V_2O_5 content. The grain size increases with the increase of V_2O_5 content from 1.5 μm for pure sample to 6.4 μm for 1.5 wt.% addition. This enhancement of grain growth can play a significant role in the conductivity of the samples which might have an influence on the dielectric property of the samples due to the activity of larger conductive grains at the higher-frequency range. At lower frequency, the charge carriers are accumulated in grain boundaries, which may be related to an increase in the permittivity of the materials resulting in high value of ε'. However, ε' remains constant at higher frequencies because the electron exchange between Fe^{2+} and Fe^{3+} cannot follow the applied AC field due to lag of hopping frequency of electrons with the applied frequency.[24,25] It is also observed that the values of ε' are reduced with the addition of V_2O_5 content at the lower-frequency region, which may be related to the decrease of hopping of electrons between Fe^{2+} and Fe^{3+} ions at octahedral sites in the ferrite matrix.[26] The dielectric constant ε' of the ferrites is dependent on the space charge polarization, which is governed by the hopping exchange of the charges between the localized states. According to Verwey and de Boer, the electronic exchange ($Fe^{2+} \leftrightarrow Fe^{3+}$) occurs at the crystallographic equivalent site without any change of the energy state of the crystal resulting in transition.[27] The hopping of electrons takes place at the octahedral site (*B*-site) and the amount of iron (Fe^{3+}) ions is mainly responsible for the hopping of electronic exchange between the localized sites. Because of the addition of V_2O_5, V^{5+} ions occupy at the *B*-site resulting in the reduction of Fe^{3+} ions, that ultimately limits the degree of electronic exchange ($Fe^{2+} \leftrightarrow Fe^{3+}$). Therefore, the probability of interfacial polarization decreases with the addition of V_2O_5 content and consequently, reduces the electron exchange between Fe^{2+} and Fe^{3+} at the *B*-site, resulting in the decrease of the dielectric constant ε'.

Figure 3 illustrates the variations of dielectric loss factor (tan δ_E) with applied frequency. It is observed that tan δ_E decreases with the increase of frequency. The higher value of tan δ_E at lower-frequency region is observed due to the grain boundary effect which requires more energy for the exchange of electron between Fe^{2+} and Fe^{3+} ions. However, the lower value of tan δ_E is observed at the higher-frequency region, which could be related to the inability of domain wall motion with the rapid variation of applied AC field. It can also be found that tan δ_E decreases with the increase of V_2O_5 content at lower frequency, which could be ascribed to the enhancement of the electrical resistivity of V_2O_5-added Ni–Co–Zn ferrites.

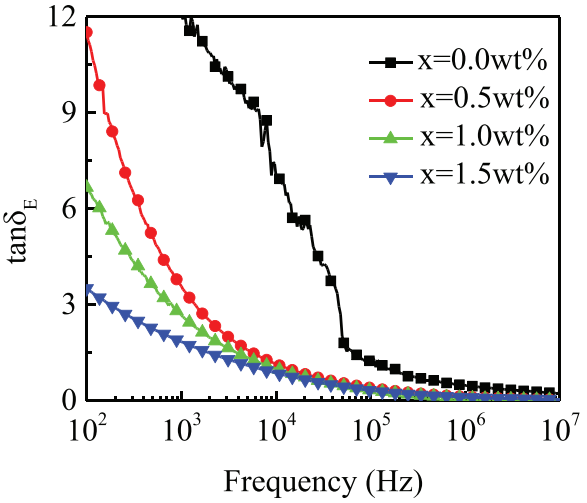

Fig. 3. Variations of the dielectric loss factor (tan δ_E) with applied frequency.

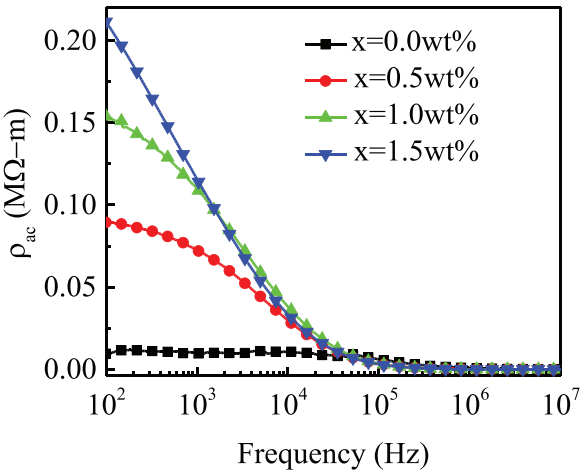

Fig. 4. Variations of ρ_{ac} with applied frequency.

3.2. *AC conductivity and resistivity*

The variations of AC electrical resistivity (ρ_{ac}) with the applied frequency are presented in Fig. 4. It shows that ρ_{ac} decreases continuously with the increase of frequency and becomes independent of frequency at higher-frequency range. It is also observed from Figs. 2 and 4 that ε' and ρ_{ac} due to the addition of V_2O_5 content are in inverse relationship with each other, which shows the normal trend of ferrites. The hopping lengths L_A and L_B were calculated[28] for the tetrahedral site and the octahedral site, respectively, and are tabulated in Table 1. Both L_A and L_B increase with the addition of V_2O_5 in Ni–Co–Zn ferrites. The electrical resistivities of V_2O_5-added Ni–Co–Zn ferrites at a selected frequency (100 Hz) are shown in Table 1. It shows that the resistivity was found to increase with the amount of V_2O_5 content, which may be related to the increase in hopping length at the octahedral site (L_B).

Table 1. Resistivity (ρ_{ac}), hopping length of tetrahedral *A*-site (L_A) and hopping length of octahedral *B*-site (L_B) for different compositions.

Composition	ρ_{ac}(MΩ · m) (at 100 Hz)	L_A (Å)	L_B (Å)
$Ni_{0.62}Co_{0.03}Zn_{0.35}Fe_2O_4$ + 0 wt.% V_2O_5	0.01	3.627	2.9620
$Ni_{0.62}Co_{0.03}Zn_{0.35}Fe_2O_4$ +0.5 wt.% V_2O_5	0.08	3.629	2.9634
$Ni_{0.62}Co_{0.03}Zn_{0.35}Fe_2O_4$ +1 wt.% V_2O_5	0.16	3.630	2.9641
$Ni_{0.62}Co_{0.03}Zn_{0.35}Fe_2O_4$ +1.5 wt.% V_2O_5	0.21	3.631	2.9648

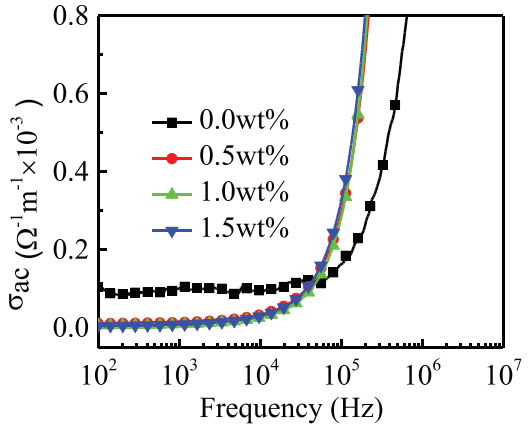

(a)

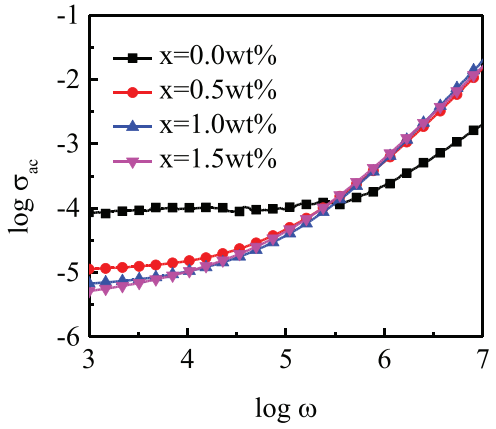

(b)

Fig. 5. (a) σ_{ac} versus frequency and (b) log σ_{ac} versus log ω.

The AC conductivities (σ_{ac}) of the studied samples as a function of frequency are shown in Fig. 5(a). It shows that σ_{ac} is almost independent of frequency at the lower-frequency region, which corresponds to DC conductivity (σ_{dc}). On the other hand, σ_{ac} increases rapidly at the higher-frequency region, called as the hopping region due to the effectiveness of conductive grains. It is also seen that σ_{ac} was reduced due to the addition of V_2O_5 in Ni–Co–Zn ferrites at lower-frequency region, which could be attributed to the increase of hopping length (L_B) and reduction of the mobility of charge carriers.[29] According to Jonscher's power law,[30] the total conductivity is given by: $\sigma_{total}(\omega) = \sigma_{dc} + B\omega^n$, where $\omega(=2\pi f)$ is the frequency, n is the dimensionless exponent quantity, which gives the information about the conduction mechanism of the samples, and $B\omega^n$ represents the AC conductivity term due to hopping process at the octahedral site.[31] Figure 5(b) shows the relation between log σ_{ac} and log ω for all the samples at room temperature. The value of n can be obtained from the slope of log σ_{ac} versus logω plot. It is found to be in the range of $0 < n < 1$ which confirms that the conduction of the samples is dependent on the frequency.[32] According to Jonscher's power law, the variation of log σ_{ac} with logω should be a linear relation. However, the conductivity of the samples shows a plateau-like shape at the low-frequency region due to mixed polaron hopping. On the other hand, it demonstrates that conductivity increases linearly at the higher-frequency region, which could be attributed to the small polaron hopping, which is responsible for the material conduction. Therefore, the enhancement of the electrical conductivity is clearly reflected by the hopping mechanism.

3.3. *Complex impedance spectra and Cole–Cole plot*

Impedance spectroscopy is a vital tool to know about the conduction mechanism of the materials. In order to study the electrical properties of V_2O_5-added Ni–Co–Zn mixed ferrites, the room-temperature complex impedance spectra were measured for all the samples. Figure 6 shows the variations of the real (Z') and imaginary (Z'') parts of impedance with applied frequency. It is observed from Fig. 6(a) that Z' decreases with increasing frequency and it remains almost constant at high frequencies. The values of Z' are increased with the addition of V_2O_5 in Ni–Co–Zn ferrites at the low-frequency region. The frequency dependence of Z'' is shown in Fig. 6(b). It shows relaxation peaks due to the presence of space charge relaxation behavior in the material. The values of Z' and Z'' both tend to merge in the high-frequency region, which may be related to the reduction of space charge polarization resulting in the increase of σ_{ac} with frequency.[33]

In general, the Cole–Cole plot (Z'' versus Z') or the Nyquist plot exhibits three successive semicircles for the effects of grain, grain boundary and surface electrode, respectively.[34] The semicircle at low-frequency region represents the resistance of the grain boundary, while the semicircle at high-frequency region is for the resistance of the grain. For an ideal Debye-type relaxation, a perfect semicircle will be seen with its center at the Z'-axis.[35] The complex impedance can be expressed as[36]: $Z^* = R_g - \frac{1}{j\omega_g C_g} + R_{gb} - \frac{1}{j\omega_{gb} C_{gb}}$, where R_g and R_{gb} are the grain and grain boundary resistances, C_g and Cgb are the grain and grain boundary capacitances, while ω_g and ω_{gb} are the frequencies at the peak of the semicircle for the grain and the grain boundary, respectively. Figure 7 shows the Cole–Cole plot for different compositions. In this investigation, it is observed that all samples display a single

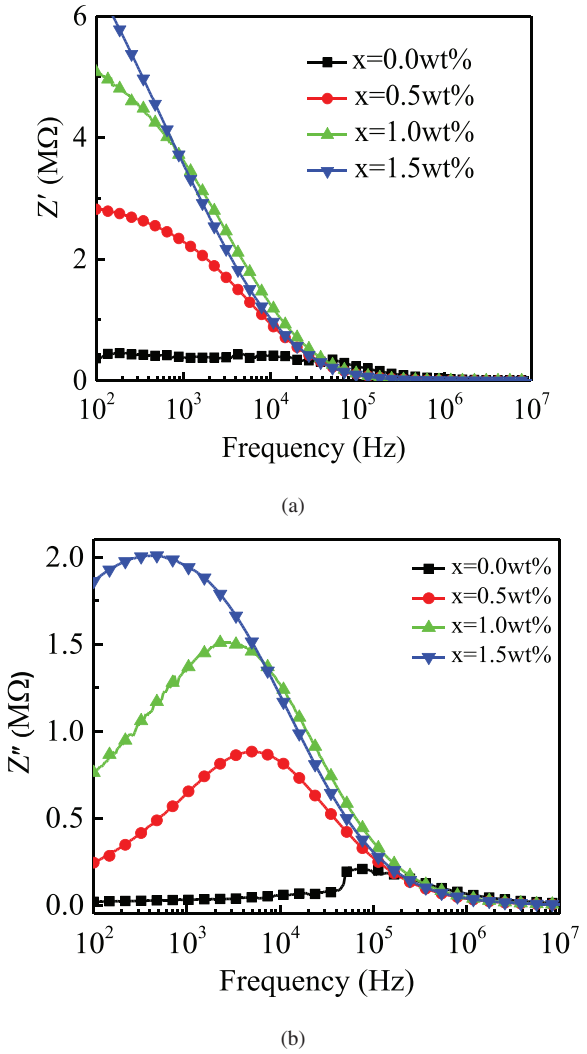

Fig. 6. (a) Z' versus frequency and (b) Z'' versus frequency.

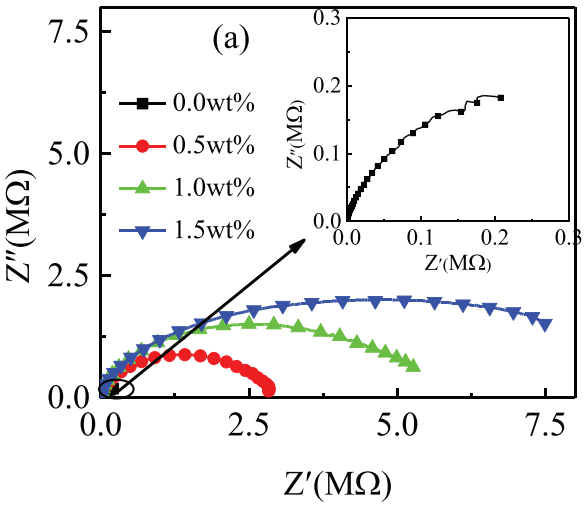

Fig. 7. Cole–Cole plot.

semicircular arc. A single semicircle indicates that only one primary mechanism is responsible for the conduction mechanism within the samples. On the other hand, the FESEM micrographs of the samples clearly demonstrated that the grain size increases with the addition of V_2O_5 content and it has been reported in our earlier work.[37] The diameter of the semicircular arc increases with increasing V_2O_5 content which signifies that the grain/bulk resistance increases with V_2O_5 addition.[38] This may be related to the larger grain size due to the addition of V_2O_5 into the Ni–Co–Zn ferrites. The result suggests that the conduction mechanism occurs predominantly through the grain property in the samples.

4. Conclusion

$Ni_{0.62}Co_{0.03}Zn_{0.35}Fe_2O_4 + xV_2O_5$ (where x = 0, 0.5, 1 and 1.5 wt.%) ferrite samples have been prepared by solid-state reaction technique. The dielectric property of V_2O_5-added Ni–Co–Zn ferrites follows the Maxwell–Wagner polarization model. The dielectric constants were reduced due to limitation of the degree of electronic exchange ($Fe^{2+} \leftrightarrow Fe^{3+}$) with the addition of V_2O_5 content at lower-frequency region. The conduction mechanism is mediated by the electron hopping between Fe^{2+} and Fe^{3+} in the spinel lattices. The AC conductivity was reduced with the addition of V_2O_5 content, which can be linked to an increase in hopping length (L_B). The analysis of complex impedance indicates that the areas under the semicircles of the Nyquist plots were increased due to the larger grain size of V_2O_5-added Ni–Co–Zn ferrites. It is inferred from the experimental evidences that conduction occurs through the grain in V_2O_5-added Ni–Co–Zn ferrites.

Acknowledgments

The authors are thankful to the Department of Physics, BUET, and the Ministry of Science and Technology, Bangladesh, and also to the Materials Science Division, Atomic Energy Center, Dhaka, for their technical support to carry out this research work.

References

[1]M. H. Rashid, M. N. Islam, M. Arifuzzaman and A. K. M. Hossain Akther, Effect of sintering temperature on the structural, morphological, electrical, and magnetic properties of Ni-Cu-Zn and Ni-Cu-Zn-Sc ferrites, *J. Mater. Sci., Mater. Electron.* **32**, 2505 (2021).

[2]N. Jahan, M. N. I. Khan, F. U. Z. Chowdhury, A. K. M. Akhter Hossain, S. M. Hoque, M. A. Matin, M. N. Hossain, M. M. Hossain and M. M. Uddin, Influence of Yb^{3+} on the structural, electrical and optical properties of sol–gel synthesized Ni-Zn nanoferrites, *Results Phys.* **19**, 103450 (2020).

[3]K. Qian, Z. Yao, H. Lin, J. Zhou, A. A. Haidry, T. Qi, W. Chen and X. Guo, The influence of Nd substitution in Ni-Zn ferrites for the improved microwave absorption properties, *Ceram. Int.* **46**, 227 (2020).

[4]M. A. Ali, M. N. I. Khan, F. U. Z. Chowdhury, M. M. Hossain, M. Z. Rahman, S. M. Hoque, M. A. Matin and M. M. Uddin, Study of physical properties towards optimizing sintering temperature of Y substituted Mg-Zn ferrites, *Results Phys.* **14**, 102517 (2019).
[5]S. Manjura Hoque, M. Samir Ullah, F. A. Khan, M. A. Hakim and D. K. Saha, Structural and magnetic properties of Li-Cu mixed spinel ferrites, *Physica B* **406**, 1799 (2011).
[6]Md. Sazzad Hossain, S. Manjura Hoque, S. I. Liba and S. Choudhury, Effect of synthesis methods and a comparative study of structural and magnetic properties of zinc ferrite, *AIP Adv.* **7**, 105321 (2017).
[7]K. Chandra Babu Naidu and W. Madhuri, Microwave assisted solid state reaction method: Investigation on electrical and magnetic properties NiMgZn ferrites, *Mater. Chem. Phys.* **181**, 432 (2016).
[8]X. Huang, J. Zhang, M. Lai and T. Sang, Preparation and microwave absorption mechanisms of the NiZn ferrite nanofibers, *J. Alloys Compd.* **627**, 367 (2015).
[9]J. S. Ghodake, R. C. Kambale, S. V. Salvi, S. R. Sawant and S. S. Suryavanshi, Electric propeties of Co substituted Ni-Zn ferrites, *J. Alloys Compd*. **486**, 830 (2009).
[10]J. S. Ghodake, R. C. Kambale, T. J. Shinde, P. K. Maskar and S. S. Suryavanshi, Magnetic and microwave absorbing properties of Co^{2+} substituted nickel-zinc ferrites with the emphasis on initial permeability studies, *J. Magn. Magn. Mater.* **401**, 938 (2016).
[11]M. D. Hossain, M. N. I. Khan, A. Nahar, M. A. Ali, M. A. Matin, S. M. Hoque, M. A. Hakim and A. T. M. K. Jamil, Tailoring the properties of Ni-Zn-Co ferrites by Gd^{3+} substitution, *J. Magn. Magn. Mater.* **497**, 165978 (2020).
[12]A. Yadav and D. Varshney, Structural and dielectric properties of copper substituted Mg-Zn spinel ferrites, *J. Supercond. Nov. Magn.* **30**, 1297 (2017).
[13]B. Ramesh, S. Ramesh, R. Vijaya Kumer and M. Lakshmipathi Rao, AC impedance studies on $LiFe_{5-x}Mn_xO_8$ ferrites, *J. Alloys Compd.* **513**, 289 (2012).
[14]J. Du, G. Yao, Y. Liu, J. Mia and G. Zu, Influence of V_2O_5 as an effective dopant on the sintering behavior and magnetic properties of $NiFe_2O_4$ ferrite ceramics, *Ceram. Int.* **38**, 1707 (2012).
[15]H. Su, H. Zhang and X. Tang, Effects of Bi_2O_3-WO_3 additives on sintering behaviors and magnetic properties of NiCuZn ferrites, *Mater. Sci. Eng. B* **117**, 231 (2005).
[16]B. Parvatheeswara Rao, O. Caltun, I. Dumitru and L. Spinu, Complex permeability spectra of Ni-Zn ferrites doped with V_2O_5/Nb_2O_5, *J. Magn. Magn. Mater.* **304**, 749 (2006).
[17]F. Xu, X. Shi, Y. Liao, J. Li and J. Hu, Investigation of grain growth and magnetic properties of low sintered LiZnTi ferrite-ceramic, *Ceram. Int.* **46**, 14669 (2020).
[18]R. Lebourgeois, S. Duguey, J.-P. Ganne and J.-M. Heintz, Influence of V_2O_5 on the magnetic properties of nickel-zinc-copper, *J. Magn. Magn. Mater.* **312**, 328 (2007).
[19]M. Kaiser, Influence of V_2O_5 ion addition on the conductivity and grain growth of Ni-Zn-Cu ferrites, *Curr. Appl. Phys.* **10**, 975 (2010).
[20]B. P. Rao, K. H. Rao, G. Sankaranarayana, A. Paduraru and O. F. Caltun, Influence of V_2O_5 additions on the resistivity and dielectric properties of nickel-zinc ferrites, *J. Optoelectron. Adv. Mater.* **7**(2), 697 (2005).
[21]G. C. Jain, B. K. Das, R. B. Tripathi and R. Narayan, Influence of V_2O_5 addition on electrical conductivity and magnetic properties of Ni-Zn ferrites, *IEEE Trans. Magn.* **18**(2), 776 (1982).
[22]B. D. Cullity, *Elements of X-ray Diffraction* (Addison-Wesley Publishing Company, MA, 1978).
[23]J. C. Maxwell, *A Treatise on Electricity and Magnetics*, Vol. 1, Chapter X, pp. 374–387 (Clarendon Press, London, 1873).
[24]R. A. Pawar, S. M. Patange, Q. Y. Tamboli, V. Ramanathan and S. E. Shirsath, Spectroscopic, elastic and dielectric properties of Ho^{3+} substituted Co-Zn ferrites synthesized by sol-gel method, *Ceram. Int.* **42**, 16096 (2016).
[25]M. Manjurul Haque, M. Huq and M. A. Hakim, Densification, magnetic and dielectric behaviour of Cu substituted Mg-Zn ferrites, *Mater. Chem. Phys.* **112**, 580 (2008).
[26]M. D. Hossain, A. T. M. K. Jamil, M. R. Hasan, M. A. Ali, I. N. Esha, M. S. Hossain, M. A. Hakim and M. N. I. Khan, Impact of V substitution on the physical properties of Ni-Zn-Co ferrites, *Mater. Res. Express* **8**, 046102 (2021).
[27]E. J. W. Verwey and J. De Boer, Cation arrangement in a few oxides with crystal structures of the spinel type, *Recl. Trav. Chim. Pays-Bas* **55**, 531 (1936).
[28]S. Nasrin, S. Mostafa Khan, M. A. Matin, M. N. I. Khan, A. K. M. Akther Hossain and M. D. Rahman, Synthesis and deciphering the effects of sintering temperature on structural, elastic, dielectric, electric and magnetic properties of magnetic $Ni_{0.25}Cu_{0.13}Zn_{0.62}Fe_2O_4$ ceramics, *J. Mater. Sci., Mater. Electron.* **30**, 10722 (2019).
[29]B. C. Das, F. Alam and A. K. M. Akther Hossain, The crystallographic, magnetic, and electrical properties of Gd^{3+} substituted Ni-Cu-Zn mixed ferrites, *J. Phys. Chem. Solids* **142**, 109433 (2020).
[30]A. K. Jonscher, The 'universal' dielectric response, *Nature* **267**, 673 (1977).
[31]S. A. Mazen and N. I. Abu Sayed, Dielectric properties and impedannce analysis of polycrystalline Li-Si ferrite prepared by high energy ball milling technique, *J. Magn. Magn. Mater*. **442**, 72 (2017).
[32]M. K. Das, M. A. Zubair, H. Tanaka and A. K. M. Akther Hossain, Study of impedance and magneto electric property of lead free xLCNZFO+$(1-x)$BGTDO multiferroic composites, *Mater. Chem. Phys.* **255**, 123575 (2020).
[33]M. A. Dar, K. M. Batoo, V. Verma, W. A. Siddiqui and R. K. Kotnala, Synthesis and characterization of nano-sized pure and Al-doped lithium ferrite having high value of dielectric constant, *J. Alloys Compd.* **493**, 553 (2010).
[34]N. J. Kidner, N. H. Perry, T. O. Mason and E. J. Garboczi, The brick layer model revisited: Introducing the nano-grain composite model, *J. Am. Ceram. Soc.* **91**(6), 1733 (2008).
[35]S. Nasrin, M. Sharmin, M. A. Matin, A. K. M. Akther Hossain and M. D. Rahman, Study the impact of sintering temperature on electromagnetic properties of $(1-y)[Ba_{0.9}Ca_{0.1}Zr_{0.1}Ti_{0.9}O_3]$ + $y[Ni_{0.25}Cu_{0.13}Zn_{0.62}Fe_2O_4]$ composites, *Appl. Phys. A* **127**, 59 (2021).
[36]M. Belal Hossen and A. K. M. Akther Hossain, Complex impedance and electric modulus studies of magnetic ceramic $Ni_{0.27}Cu_{0.10}Zn_{0.63}Fe_2O_4$, *J. Adv. Ceram.* **4**(3), 217 (2015).
[37]M. Samir Ullah, M. Firoz Uddin, A. A. Momin and M. A. Hakim, Effect of V_2O_5 addition on the structural and magnetic properties of Ni–Co–Zn ferrites, *Mater. Res. Express* **8**(1), 016102 (2021).
[38]P. P. Hankare, R. P. Patil, U. B. Sankpal, K. M. Garadkar, R. Sasikala, A. K. Tripathi and I. S. Mulla, Magnetic, dielectric and complex impedance spectroscopic studies of nanocrystalline Cr substituted Li-ferrite, *J. Magn. Magn. Mater*. **322**, 2629 (2010).